Carcinogenesis vol.33 no.9 pp.1736–1744, 2012
doi:10.1093/carcin/bgs204
Advance Access Publication June 10, 2012

Dysregulation of miR-31 and miR-21 induced by zinc deficiency promotes esophageal cancer

Hansjuerg Alder[1,†], Cristian Taccioli[1,6,†], Hongping Chen[2,†], Yubao Jiang[2], Karl J. Smalley[3], Paolo Fadda[1], Hatice G. Ozer[4], Kay Huebner[1], John L. Farber[5], Carlo M. Croce[1] and Louise Y.Y. Fong,[2,3,*]

[1]Department of Molecular Virology, Immunology, and Medical Genetics, Comprehensive Cancer Center, The Ohio State University, Columbus, OH, 43210, USA, [2]Department of Pharmacology & Experimental Therapeutics, Thomas Jefferson University, Philadelphia, PA, 19107, USA, [3]Kimmel Cancer Center, Thomas Jefferson University, PA, 19107, USA, [4]Biomedical Informatics, Ohio State University, Columbus, OH, 43210, USA, [5]Department of Pathology, Anatomy & Cell Biology, Thomas Jefferson University, Philadelphia, PA, 19107, USA and [6]Current address: Department of Cancer Biology, Paul O'Gorman Cancer Institute, University College London, London WC1E 6B, UK

*To whom correspondence should be addressed. Tel: 215 955 5616;
Fax: 215 955 7006;
Email: Louise.Fong@Jefferson.edu
Correspondence may also be addressed to Carlo M. Croce, Tel: 614 292 3063;
Fax: 614 292 3558;
Email: Carlo.Croce@osumc.edu

Zinc deficiency (ZD) increases the risk of esophageal squamous cell carcinoma (ESCC). In a rat model, chronic ZD induces an inflammatory gene signature that fuels ESCC development. microRNAs regulate gene expression and are aberrantly expressed in cancers. Here we investigated whether chronic ZD (23 weeks) also induces a protumorigenic microRNA signature. Using the nanoString technology, we evaluated microRNA profiles in ZD esophagus and six additional tissues (skin, lung, pancreas, liver, prostate and peripheral blood mononuclear cells [PBMC]). ZD caused overexpression of inflammation genes and altered microRNA expression across all tissues analyzed, predictive of disease development. Importantly, the inflammatory ZD esophagus had a distinct microRNA signature resembling human ESCC or tongue SCC miRNAomes with *miR-31* and *miR-21* as the top-up-regulated species. Circulating *miR-31* was also the top-up-regulated species in PBMCs. In ZD esophagus and tongue, oncogenic *miR-31* and *miR-21* overexpression was accompanied by down-regulation of their respective tumor-suppressor targets PPP2R2A and PDCD4. Importantly, esophageal *miR-31* and *miR-21* levels were directly associated with the appearance of ESCC in ZD rats, as compared with their cancer-free Zn-sufficient or Zn-replenished counterparts. In situ hybridization analysis in rat and human tongue SCCs localized *miR-31* to tumor cells and *miR-21* to stromal cells. In regressing tongue SCCs from Zn-supplemented rats, *miR-31* and *miR-21* expression was concomitantly reduced, establishing their responsiveness to Zn therapy. A search for putative microRNA targets revealed a bias toward genes in inflammatory pathways. Our finding that ZD causes *miR-31* and *miR-21* dysregulation associated with inflammation provides insight into mechanisms whereby ZD promotes ESCC.

Introduction

Oral-esophageal squamous cell carcinomas (OSCC, ESCC) are major causes of cancer deaths worldwide. Because of absence of early symptoms, ESCC is frequently diagnosed at an advanced stage and has a 5-year survival of 10%. Patients with OSCC (major site, tongue) have a high mortality rate, because of the appearance of second cancers in the esophagus through field cancerization effects (1). Despite the decline in worldwide cancer-mortality rates since the mid 1980s, ESCC and OSCC remain deadly diseases. Thus, clarification of their pathogenesis and development of new prevention strategies are urgently needed.

The major risk factors for developing oral-esophageal carcinomas include alcohol consumption, tobacco use and nutritional deficiencies. Epidemiological and clinical studies have implicated dietary zinc (Zn) deficiency (ZD) in the pathogenesis of ESCC and OSCC (2,3). Zn is an essential trace element required for the activity of >300 enzymes, for proper immune function and for the conformation of >2000 transcription factors that control cell proliferation, apoptosis and signaling pathways (4). ZD predisposes to diseases by adversely affecting these processes.

Our ZD rat oral-esophageal cancer model reproduces the ZD link to human ESCC and OSCC (5) and provides a unique opportunity to decipher the mechanism by which ZD promotes oral-esophageal carcinogenesis. Previously, we showed that weanling rats on a ZD diet for 6 weeks developed a precancerous condition in the upper aerodigestive tract (tongue, esophagus and forestomach [expanded lower esophagus]), with increased cellular proliferation (5) and extensive gene-expression changes, including overexpression of proinflammation genes *S100 calcium binding protein a8 and a9* (*S100a8 and S100a9*) (6). Subsequently, prolonged ZD (21 weeks) was shown to amplify this inflammation in the esophagus by causing overexpression of numerous inflammation genes in addition to *S100a8/S100a9*, thereby providing an inflammatory microenvironment conducive to ESCC development on repeated exposure to the environmental carcinogen *N*-nitrosomethylbenzylamine (NMBA). Zn replenishment (ZR) reversed the inflammatory signature and prevented cancer formation (7). In addition, Zn supplementation in nutritionally complete rats suppressed tongue SCC development by attenuating the inflammation (8).

microRNAs (miRNAs) are a family of short noncoding RNAs that have emerged as powerful posttranscriptional regulators of gene expression (9). The ability of individual miRNAs to regulate a large number of mRNA species allows them to coordinate complex programs of gene expression that alter a range of biological processes, including cellular proliferation, apoptosis, immune response and signaling events (10). miRNAs expression levels are altered in many types of human cancer, including ESCC and OSCC (11). Furthermore, miRNA expression patterns are associated with chronic inflammatory diseases and other inflammatory conditions (12).

We asked whether overexpression of cancer-related inflammation genes induced by ZD in the rat esophagus (7) is a consequence of a protumorigenic miRNA signature. For this, we examined miRNA profiles in esophagus and six additional tissues (skin, lung, pancreas, liver, prostate and peripheral blood mononuclear cells [PBMC]) after chronic ZD (23 weeks) using the novel nanoString nCounter technology (Seattle, WA) (13,14). The deficient esophagus exhibited a prooncogenic miRNA signature with *miR-31* and *miR-21* as the top-up-regulated species. The role of these two oncomiRs in esophageal and oral neoplasia was further explored. ZD also induced distinct miRNA expression patterns across all tissues profiled.

Materials and methods

Animals

Male weanling male Sprague-Dawley rats were obtained from Taconic Laboratory (Germantown, NY). Custom-formulated egg-white-based diets were from Harlan Teklad (Madison, WI). ZD- and Zn-sufficient (ZS) diets were identical except for the Zn content, which was 3–4 ppm and 65 ppm, respectively.

Abbreviations: BCIP, 5-brom-4-chloro-3′-indolylphosphate; DAVID, Database for Annotation, Visualization and Integrated Discovery; ESCC, esophageal squamous cell carcinoma; FFPE, formalin fixed and paraffin embedded; GO, gene ontology; IHC, immunohistochemistry; ISH, in situ hybridization; miRNAs, microRNAs; NBT, 4-nitro-blue tetrazolium; PBMC, peripheral blood mononuclear cells; Zn, zinc; ZD, Zn deficient; ZS, Zn sufficient, ZR, Zn replenished.

[†]These authors contributed equally to this work.

Experimental design

The animal study was conducted according to approved Institutional animal protocols. Weanling rats (n = 19) were fed *ad libitum* a ZD diet for 23 weeks. Control rats (n = 15) were pair fed a ZS diet to match the decreased food consumption of ZD animals (7). At study conclusion, blood was collected from the retro-orbital venous plexus after anesthesia with isoflurane. PBMCs were prepared from whole blood using Histopaque-1077 (Sigma-Aldrich, St Louis, MO). Esophagus, tongue, skin, lung, liver, prostate and pancreas were isolated. Esophagus and tongue were cut into two portions. One portion was formalin fixed and paraffin embedded (FFPE) for histological, immunohistochemical (IHC), and in situ hybridization (ISH) studies. Esophageal and tongue mucosa were prepared as previously described (15). The prostate was microdissected into dorsal, lateral, ventral and anterior lobes. Tissues were snap frozen in liquid nitrogen and stored at –80°C.

RNA preparation

Total RNA was prepared using TRIZOL reagent (Invitrogen, Carlsbad, CA) (7).

miRNA expression profiling

The multiplexed nanoString nCounter miRNA system (nanoString Technologies) (13,14) was used for miRNA expression profiling in esophagus and six additional tissues (skin, lung, pancreas, liver, prostate and PBMC; n = 6 rats/tissue/dietary group). This assay was performed at the Ohio State University Comprehensive Cancer Center Nucleic Acid Facility.

Total RNA (100 ng) was used as input material. Small RNA samples were prepared by ligating a specific DNA tag onto the 3' end of each mature miRNA according to manufacturer's instruction (nanoString Technologies). These tags normalized the melting temperatures (Tms) of the miRNAs and provided identification for each miRNA species in the sample. Excess tags were then removed and the resulting material was hybridized with a panel of miRNA:tag-specific nCounter capture and barcoded reporter probes. Hybridization reactions were incubated at 64°C for 18 h. Hybridized probes were purified and immobilized on a streptavidin-coated cartridge using the nCounter Prep Station (nanoString Technologies). nCounter Digital Analyzer was used to count individual fluorescent barcodes and quantify target RNA molecules present in each sample. For each assay, a high-density scan (600 fields of view) was performed.

nanoString data analysis

Abundances of miRNAs were quantified using the nanoString nCounter gene-expression system (13). Each sample was normalized to the geometric mean of the top 50 most highly expressed miRNAs. Student's t-test was used to calculate statistical significances of pair-wise comparisons. Calculations were performed using the *R* statistical computing environment (http://www.r-project.org/).

Gene ontology (GO) analysis

GO analysis was performed using miRNAs with $P < 0.05$ and fold change of >1.3. For each miRNA, the common target genes found in two or more databases (RNAhybrid, TargetScan, miRDB and microRNA.org) were used. GO analysis was then performed for each tissue using DAVID (Database for Annotation, Visualization and Integrated Discovery) (16).

TaqMan miRNA assay

TaqMan miRNA assays was performed to quantify mature miRNAs using predesigned probes, rat U87 as the normalizer (Applied Biosystems, Foster City, CA), and the comparative C_t method. Real-time PCR was performed on the ABI Prism 7900HT Sequence detection system (Applied Biosystems).

ISH

miRCURY locked nucleic acid (LNA) microRNA detection probes, namely, rno-miR-21, rno-miR-31, hsa-miR-31, negative controls (rno-miR-31 and rno-miR-21) with mismatches at two positions, were purchased from Exiqon (Vedbaek, Denmark). The oligonucleotides are double DIG-labeled at the 5'- and 3'-ends. ISH was performed on 6 µm FFPE sections as described by Nielsen *et al*. (17). Following deparaffinization, rehydration in graded alcohol and proteinase K treatment, tissue sections were hybridized with miR-31 probe (20 nM), or *miR-21* probe (50 nM) in hybridization buffer (Exiqon) at 57°C for 14 h in a hybridizer (Dako, Glostrup, Denmark). Following stringent washes in SSC buffers, the sections were blocked against unspecific binding of the detecting antibody, using DIG wash and blocking reagent. miRNA was localized by incubation with 4-nitro-blue tetrazolium (NBT) and 5-brom-4-chloro-3′-indolylphosphate (BCIP; Roche, Mannheim, Germany). Nuclear fast red (Vector Lab., Burlingname, CA) was used as a counterstain.

Quantitative real time PCR

qRT-PCR was performed using predesigned probes (Applied Biosystems), PSMB6 as the normalizer and the comparative C_t method (7).

IHC

IHC was performed on esophageal/lingual sections to assess nuclear programmed cell death 4 (PDCD4; LS-B1388, Lifespan Biosciences, Seattle, WA) after citrate-based antigen retrieval as previously described (7). Protein was localized by incubation with 3-amino-9-ethylcarbazole substrate-chromogen (AEC; Dako, Carpinteria, CA).

Immunoblot analysis

Total protein samples were separated by SDS-polyacrylamide gel electrophoresis and transferred onto polyvinylidene difluoride membranes (7). After incubation with primary antibodies: PDCD4 (LS-B1388, Lifespan Biosciences), TPM1 (ab55915; Abcam, Cambridge, MA), PPP2R2A (#5689, Cell Signaling, Danvers, MA). RHOBTB1 (sc-102084; Santa Cruz Biotech, CA), STAU2 (sc-87439; Santa Cruz Biotech) and loading control GAPDH (CB1001, Calbiochem, San Diego, CA), the membrane was incubated with appropriate peroxidase-conjugated secondary antibodies. Immunodetection was by Pierce enhanced chemiluminescence substrate (Thermo Scientific, Waltham, MA) and intensity of protein bands quantified by GS-800 calibrated densitomter (BIO-RAD, Hercules, CA).

Zn measurement

Tissue Zn content was determined using Atomic Absorption Spectrometer Analyst 400 (PerkinElmer, Waltham, MA).

Rat and human tongue SCC samples

Archived rat tongue SCC tissues (FFPE) were derived from a previous study (8). Human tongue SCC tissues (FFPE) were from Thomas Jefferson University Hospital.

Rat ESCC samples

Archived rat ESCC tissues (FFPE) and RNAs were derived from a previous study (7).

Statistical analysis

Differences in Zn, gene expression and protein levels were assessed with Student's t-test. Statistical tests were two-sided and were considered significant at $P < 0.05$.

Results

Prolonged ZD reduces tissue Zn levels and induces overexpression of inflammation genes

Chronic dietary ZD (23 weeks) led to a significant decline in Zn levels across all tissue types (Figure 1A). Zn levels in serum and testis (two widely used indicators of ZD) were 52% and 40% lower in ZD than control ZS rats. Prostate accumulates the most Zn under normal condition (18) showed the greatest decline in tissue Zn levels (–53%), followed by esophagus (–47%), skin (–43%), pancreas (–42%), tongue (–33%) and lung (–26%). Liver showed the least reduction (–19%).

Chronic ZD induced up-regulation of numerous inflammatory genes in the esophagus (7). Whether it also causes inflammation in the other tissue types was evaluated by analyzing the expression of eight cancer-associated inflammation genes (*S100a8*, *S100a9*, *Cxcl5*, *Il1b, Cxcl2, Cxcr4, Ptgs2* and *Tlr4*) (7), using qRT-PCR. The ZD tongue is highly susceptible to chemically induced carcinogenesis (5) and was the only tissue that showed overexpression of all eight inflammatory genes (Figure 1B). *S100a8* and *S100a9* were overexpressed in all tissues studied (Figure 1B). In PBMC, the difference between ZD and ZS samples was suggestive but not statistically significant (*S100a8*, P = 0.07; *S100a9*, P = 0.08). Immunoblot and enzyme-linked immunosorbent assay (ELISA) analyses showed that the ZD effect observed at the transcript levels for *S100a8, S100a9, Cxcl5* and *Il1b* were also reflected at the protein level in tongue, lung and pancreas (Figure 1C and 1D). These data establish that prolonged ZD reduces Zn levels across tissue types and up-regulates expression of key inflammation genes.

Normal ZS tissues show high abundance of tissue-specific miRNAs

The nanoString platform directly measures miRNA expression levels without reverse transcription or PCR amplification, thereby eliminating enzymatic bias (13,14). At the time we initiated this study, the nanoString rat miRNA kit was unavailable. Initially, we used the human miRNA assay to profile PBMC and then the mouse miRNA assay to profile esophagus, skin, lung, pancreas, liver and

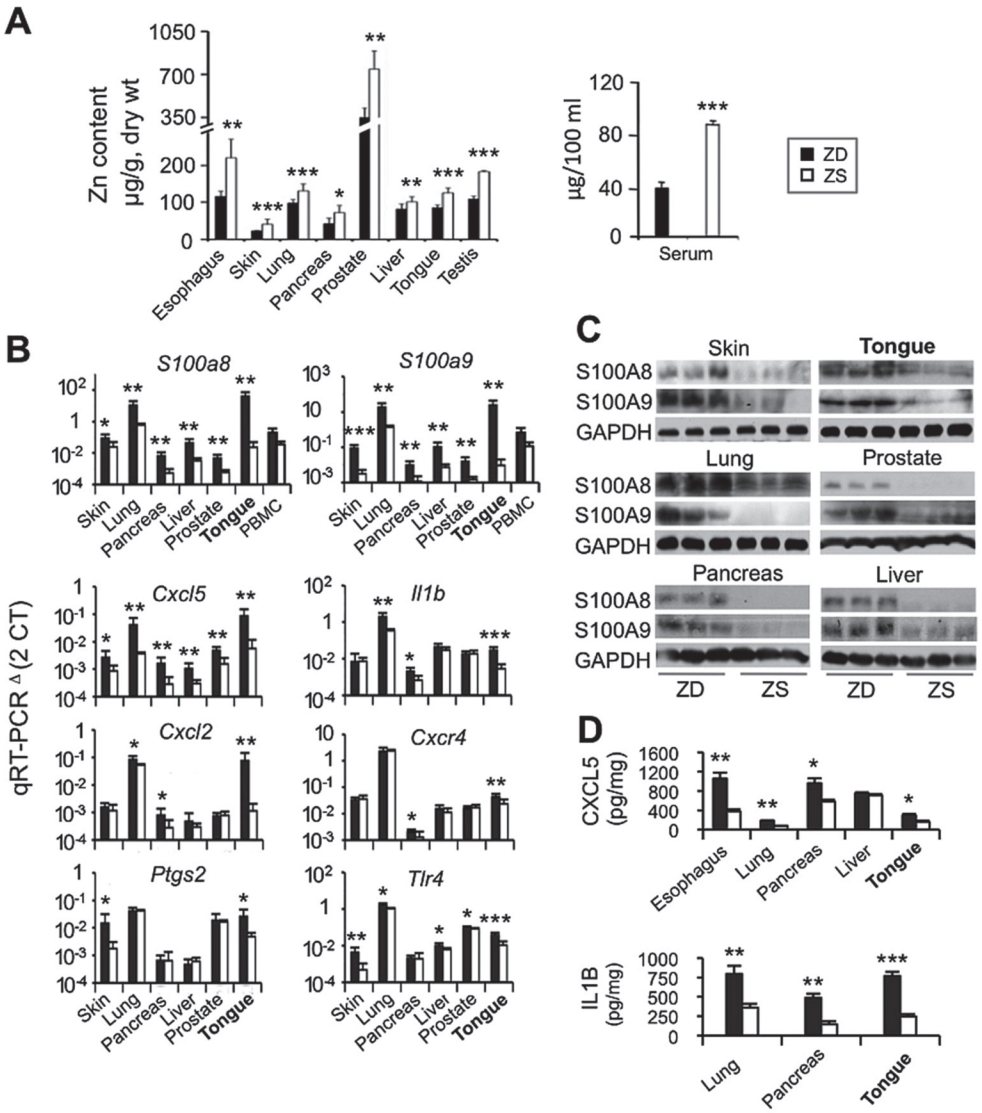

Fig. 1. Zn content and inflammation markers in ZD rat tissues. (**A**) Serum and tissue Zn content in ZD and ZS rats (*$P < 0.05$, **$P < 0.01$, ***$P < 0.001$, $n = 6$ - 8 rats/tissue). (**B**) qRT-PCR analysis of 8 inflammation genes (normalized to PSMB6, $n = 6$–8 rats/group; *$P < 0.05$, **$P < 0.01$, ***$P < 0.001$). (**C**) Expression of inflammation proteins: immunoblot (S100A8 and S100A9, $n = 3$ rats/group. (**D**) ELISA assay (CXCL5 and IL1B, $n = 3$ rats/group).

prostate. Because of a high degree of sequence conservation of miRNAs across human, mouse and rat, 178 and 236 miRNAs on the human and mouse panels, respectively, have sequences identical to the rat miRNAs. Thus, we profiled 178 rat miRNAs in PBMC and 236 rat miRNAs in the other six tissues ($n = 6$ rats/tissue/dietary group).

The nanoString profiling platform provided an estimate of miRNA abundance in normal ZS and ZD organs. ZS organs showed high abundance of many tissue-specific miRNAs (see Supplementary Table I online). As shown in Figure 2B, the liver-specific *miR-122* (19) was abundantly expressed in the liver; skin-specific *miR-203* (20) in the skin; epithelial tissue-specific *miR-205* in skin and esophagus; pancreatic islet-specific *miR-375* (21) and pancreas-specific *miR-216* and *miR-217* (22) in the pancreas; and the hematopoietic markers *miR-142-3p* (23), *miR-150*, *miR-16*, *miR191*, *miR-26a*, *miR-19b* (24) in PBMC. Conversely, the ubiquitous oncogenic *miR-21* was expressed with moderate abundance across all seven tissues, and oncogenic *miR-31* in low abundance in these same tissues. These miRNA abundance data from normal rat tissues establish that the nanoString technology is both sensitive and specific.

ZD induces a prooncogenic miRNA signature in inflammatory esophagus

Using a cutoff point of P-value <0.05 and ≥1.3 fold difference, we identified 30 dysregulated miRNAs in the inflammatory-deficient esophagus (23 up- and 7 down-regulated) (Figure 2C, see Supplementary Table II online). Importantly, the ZD esophagus had a distinct miRNA signature that resembles the miRNAomes of human ESCC and tongue SCC (25–33). This signature was defined by up-regulation of five oncogenic miRNAs (*miR*-31, 3.0 fold; *miR*-21, 2.7 fold; *miR*-223, 2.5 fold; *miR*-142-3p, 2.4 fold; *miR*-221, 1.6 fold) and down-regulation of two tumor suppressors (*miR*-204, –2.5 fold; *miR*-375, –2.0 fold). Because these same miRNAs are aberrantly expressed in human ESCC and tongue SCC (25–33), prolonged ZD induces a miRNA expression profile in the rat esophagus that in human tissue is predicative of ESCC development.

We then determined whether the top-up-regulated *miR*-31 and *miR-21* in ZD esophagus are also overexpressed in the highly tumorigenic (5) and inflammatory ZD tongue (Figure 1, B-D). Using Taqman miRNA assay (Figure 3A), both oncomiRs were significantly overexpressed in ZD tongue as compared to ZS counterpart (*miR*-31, 2.6 fold, $P = 0.013$; *miR*-21, 3.9 fold, $P = 0.014$; $n = 6$ rats/dietary

Table I. The miRNA target biological processes enrichment in Zn-deficient tissues by gene ontological (GO)

Tissue	GO terms	No. of genes	En* Score	Adjusted *P*-value
Esophagus	Zinc ion binding family	119	3.4	0.010
	Positive regulation of Cell Differentiation	67	2.9	0.011
	Serine/threonine-proteine kinase 10 family	59	1.8	0.021
	MAPKK and JNK family	42	1.4	0.041
	Negative regulation of actin filament family	31	1.3	0.042
	Epithelial cell proliferation	22	0.9	0.049
Skin	ATP calmodulin pathway	56	4.1	0.018
	Actin and ubiquitin regulation	24	2.1	0.023
	Zinc ion binding proteins	18	1.0	0.044
Lung	Transcription regulation by RNA-pol II	187	3.1	0.015
	Negative regulation of biosynthesis pathways	103	2.9	0.012
	Zinc ion binding family	68	1.4	0.037
	Lung development	23	1.0	0.046
Pancreas	Positive regulation of anti-apoptosis genes	79	2.1	0.024
	Insulin signal pathway	68	1.2	0.035
	Zinc ion binding proteins	20	0.9	0.046
Liver	Zinc ion binding family	101	4.1	0.023
	Glicosyl-lysin family	93	2.1	0.028
	Post-transcription regulation	49	1.7	0.033
Prostate	Magnesium metabolism family	77	6.4	0.021
	ATP biosynthetic process	63	5.5	0.022
	Endocytosis	39	4.9	0.033
	Transcription regulatory activity	21	3.4	0.036
	TGB-beta signaling pathway	22	2.0	0.040
	Zinc finger domain family	19	1.4	0.046
PBMC	Zinc finger family	115	3.0	0.035
	Ubiquitin-conjugating enzyme	82	2.8	0.039
	Proteolysis – cellular protein catabolic process	79	1.7	0.040
	Protein-lysin-N-methyltransferase activity	62	1.4	0.045

* Enrichment Score.

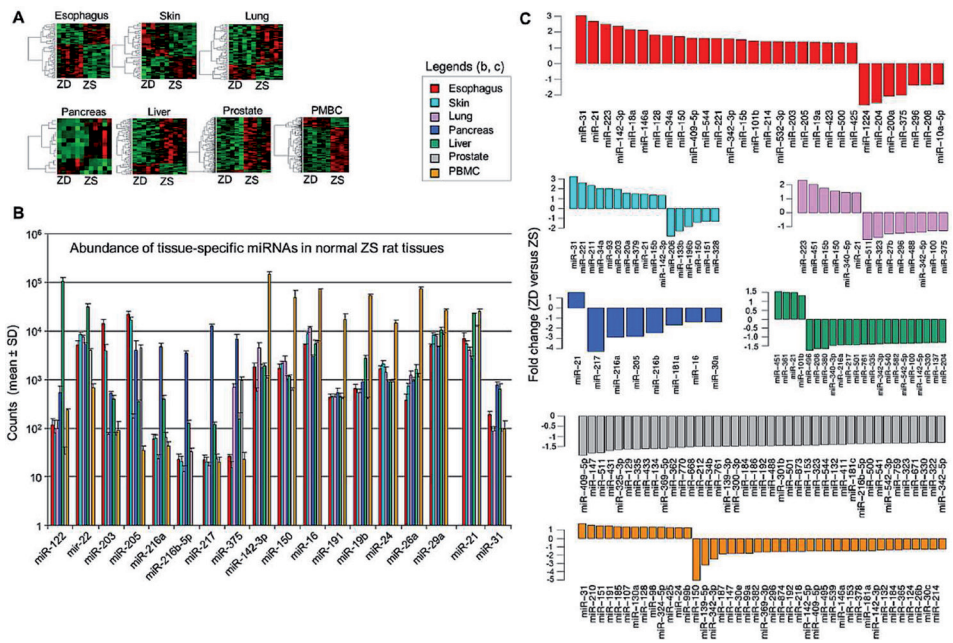

Fig. 2. miRNA expression profiles of ZD esophagus and six additional tissues. (**A**) Heat maps with supervised clustering of miRNAs expression in seven tissues. Red, green and black colors represent high, low and mean expression levels, respectively ($n = 6$ rats/dietary group/tissue, except PBMC: $n = 7$ (ZD) and 5 (ZS); $P < 0.05$). (**B**) Normal ZS tissues showing tissue-specific miRNA expression in liver, skin, pancreas and PMBC; (**C**) Barplots showing fold change of miRNA expression in 7 ZD versus ZS tissues (cutoff of $P < 0.05$, fold change ≥ 1.3).

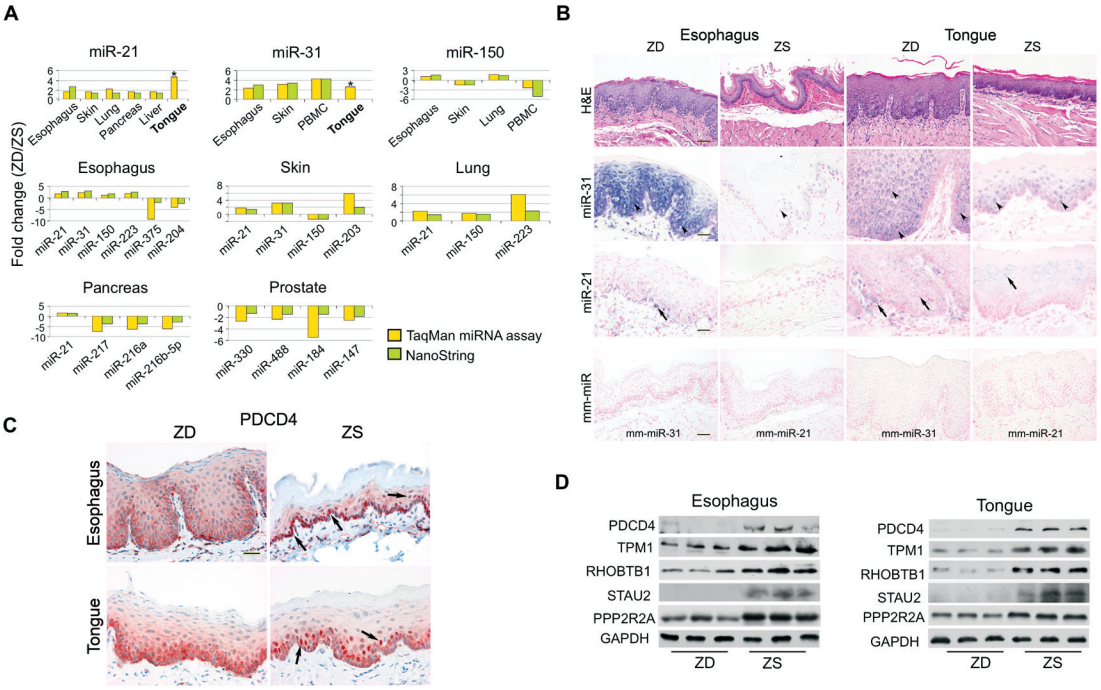

Fig. 3. Validation of nanoString miRNA profiling data. (**A**) Validation of 14 representative miRNAs in various ZD tissues and expression of miR-31 and miR-21 in ZD tongue by TaqMan miRNA assays. (**B**) ISH localization of miR-31 and miR-21 in esophagus and tongue (23 weeks ZD). miR-31 signal (arrow heads, blue, NBT/BCIP; counterstain, nuclear fast red) was strong/abundant in hyperplastic ZD esophageal and tongue epithelia versus moderate/infrequent in control ZS tissues. miR-21 signal (blue, arrows) was moderate in basal and stromal cells in ZD tissues but infrequent in ZS tissues. No ISH signal was seen with mm-*miR-31* or mm-miR-21 (two mismatches). Scale bar, 25 μm. miRNA was localized by 4-nitro-blue tetrazolium (NBT) and 5-brom-4-chloro-3′-indolylphosphate (BCIP). (**C**) IHC showing reduction of PDCD4 protein expression (nuclear) in ZD esophagus and tongue versus ZS tissues. (**D**) Immunoblots show down-regulation of PDCD4 and TPM1 protein (targets of miR-21), RHOBTB1, STAU2 and PPP2R2A protein (targets of miR-31) in ZD esophagus and tongue versus ZS tissues.

group). Thus, oncogenic *miR*-31 and *miR-21* were overexpressed in ZD tongue as in human tongue SCC (29,30,32,33).

ZD tissues have distinct miRNA profiles

In addition to esophagus, hierarchical clustering of miRNAs revealed that the other six ZD tissues had distinct miRNA profiles (Figure 2A), indicating that ZD alters miRNA expression in a tissue-specific manner. Using *P*-values <0.05 and cutoff of ≥1.3 fold difference; groups of differentially expressed miRNAs were identified in these ZD tissues (Figure 2C, see Supplementary Table II online).

Skin. Several of the up-regulated miRNAs in the inflammatory ZD skin, namely, *miR*-31 (3.3 fold), *miR-21* (1.5 fold) and *miR*-142-3p (1.3 fold), are hallmarks of the miRNAome of human psoriasis, a chronic inflammatory skin disease (34). Interestingly, ZD is implicated in the pathogenesis of psoriasis (35). As in the ZD skin (Figure 1B, 1C), psoriasis overexpresses the inflammatory mediators *S100A8* and *S100A9* (36).

Lung. We identified 14 dysregulated miRNAs in ZD lung, with *miR*-223 (2.3 fold), *miR*-451 (2.0 fold), *miR*-15b (1.8 fold) and *miR-21* (1.4 fold) among the top-up-regulated species. Importantly, these same miRNAs are overexpressed in the miRNA signatures of the inflammatory chronic obstructive pulmonary disease (COPD) (37) and lung cancers (38). Thus, prolonged ZD alters expression of specific miRNAs involved in the pathogenesis of human lung diseases.

Pancreas. Only eight miRNAs were dysregulated in ZD pancreas, including up-regulation of oncogenic *miR-21* (1.5 fold) and down-regulation of the pancreas-specific (22) *miR*-217 (-4.3 fold), *miR*-216a (-2.9 fold), *miR*-216b-5p (-2.4 fold). Importantly, *miR-21* up-regulation (38), as well as down-regulation of *miR*-216 and *miR*-217 (22) have been reported in human pancreatic ductal adenocarcinoma. In particular, *miR*-217 down-regulation was reported to discriminate normal pancreas, chronic pancreatitis and cancerous tissues (22). Thus, the ZD pancreas shows an oncogenic signature that in human tissue predisposes to pancreatic cancer.

Liver. Among the 22 dysregulated miRNAs identified in ZD liver, only oncogenic *miR-21* (1.5 fold) has been reported in human hepatocellular cancer (39).

Prostate. Zn is important for prostate health. The pathogenesis of prostate cancer involves the transformation of normal prostate epithelial cells that accumulate Zn to malignant prostate cells that do not accumulate Zn (18). ZD prostate that showed the greatest decline in Zn levels (Figure 1A) had 41 down-regulated miRNAs. Several tumor suppressors, including *miR*-184 (–1.5 fold), *miR*-488 (–1.5 fold) and *miR*-330 (–1.3 fold), are hallmarks of the human prostate cancer miRNAome (40–42).

PBMC. PMBC are leukocytes that have a round nucleus such as lymphocytes (T cells, B cells), natural killer cells and monocytes. Circulating *miR*-31 was the top-up-regulated species (1.8 fold) in PBMC from ZD versus ZS rats. Because *miR-31* was also overexpressed in ZD esophagus, tongue and skin, this result suggests an association between circulating and tissue miR-31. *miR*-150 was the most down-regulated species in PBMC of ZD rats (–5.1 fold). In patients with sepsis, *miR*-150 levels in PBMC and plasma were significantly reduced (43). In this regard, patients with sepsis are frequently ZD (44).

To summarize, dietary ZD induces dysregulation of key oncogenic and tumor-suppressor miRNAs in the esophagus and across all tissues profiled. The most shared miRNAs in signatures of the ZD tissues were oncogenic *miR-21* and *miR-31* (see Supplementary Table III online), with *miR-21* up-regulated in six (esophagus, pancreas, liver, skin, lung, tongue) and *miR*-31 in four tissues (esophagus, skin, PBMC, tongue).

Validation of nanoString profiling data

To validate the nanoString results, we performed Taqman miRNA assays on 14 selected miRNAs ($n = 6$ rats/tissue/dietary group). In all 14 cases, the same pattern and fold changes response to dietary ZD was observed using Taqman as with the nanoString assay (Figure 3A).

Taqman confirmed *miR-21* up-regulation in six ZD tissues (esophagus, skin, lung, pancreas, liver, tongue); *miR*-31 up-regulation in four ZD tissues (esophagus, skin, PBMC, tongue); *miR*-150 up-regulation in two ZD tissues (esophagus, lung) and down-regulation in circulating PBMC and skin. In addition, differential expression of representative miRNAs was validated in esophagus (up-regulation of *miR*-21, *miR*-31, *miR*-150, *miR*-223 and down-regulation of *miR*-375, *miR*-204), skin (up-regulation of *miR*-21, *miR*-31, *miR*-203; down-regulation of *miR*-150), lung (up-regulation of *miR*-21, *miR*-150, *miR*-223), pancreas (up-regulation of *miR-21* and down-regulation of *miR*-217, *miR*-216a, *miR*-216b-5p) and prostate (down-regulation of *miR*-330, *miR*-448, *miR*-184, *miR*-147). Thus, Taqman miRNA data confirm the accuracy of the nanoString data.

Cellular localization of miR-31 and miR-21 in ZD esophageal and tongue epithelia

We focused our study on the top-up-regulated *miR*-31 and *miR-21* because of their roles in human ESCC and OSCC (27,29–32). Their cellular localizations in esophageal and tongue preneoplastic tissues after chronic dietary ZD (23 weeks) was defined by performing ISH on FFPE tissues using high affinity double Dig-labeled LNA probes (Exiqon, Vedbaek, Denmark; n = 10 rats/dietary group). The hyperplastic ZD esophagus and tongue epithelial cells showed abundant *miR-31* ISH signal, as compared with nonproliferative ZS tissues (Figure 3B). In contrast, *miR-21* ISH signals were infrequent and found mostly in stromal calls of ZD tissues and were generally scarce in ZS tissues (Figure 3B). These data establish that *miR-31* and *miR-21* expression is cell-type specific with *miR-31* localized to epithelial and *miR-21* mostly in stromal cells.

miR-31 and miR-21 overexpression correlates with down-regulation of their tumor-suppressor targets

In human tongue SCC, a correlation of *miR-21* overexpression with loss of its tumor-suppressor targets PDCD4 (30) and TPM1 (45) mRNA and protein expression is documented. We determined if up-regulation of oncogenic *miR-21* in ZD tissues is accompanied by down-regulation of these two known tumor-suppressor targets. Using IHC, PDCD4 was strongly expressed in the nuclei of epithelial cells of ZS esophagus and tongue. This nuclear staining of PDCD4 was reduced or absent in the hyperplastic ZD esophagus and tongue (Figure 3C). In addition, immunoblotting analysis showed that both PDCD4 and TPM1 protein expression was markedly reduced in ZD esophagus and tongue versus ZS tissues (Figure 3D).

Using immunoblotting analysis (Figure 3D), we showed that overexpression of *miR-31* in ZD esophagus and tongue as compared with ZS tissues was associated with down-regulation of its known tumor-suppressor target PPP2R2A (46) and putative targets RHOBTB1 and STAU2 (identified by TargetScan algorithm). The putative target RHOBTB1 is a candidate tumor-suppressor gene in head and neck SCC (47) and STAU2 mRNA down-regulation was previously noted in ZD versus ZS esophagus by microarray analysis (6). Whether RHOBTB1 and STAU2 are *bona fide* targets of *miR-31* remain to be investigated.

Overexpression of miR-31 and miR-21 is associated with ESCC in ZD rats

ZD induced an inflammatory gene-expression profile that fueled ESCC in rats with repeated exposure to NMBA (7). Using qRT-PCR on archived RNA samples (7), *miR-31 and miR-21* exhibited 5.4 and 3.2-fold up-regulation in ESCC-bearing ZD rats versus cancer-free ZS controls (Figure 4A). ZR, a regimen that prevented ESCC development (7) reduced their expression to ZS levels (Figure 4A). ISH on archived FFPE tissues (7) (n = 15/dietary group) from ZD rats showed abundant *miR-31* signal in tumors/dysplastic epithelium and *miR-21* signal in tumor stroma (Figure 4B). Conversely, ISH signals of both oncomiRs were weak/absent in ZS or ZR samples (see Supplementary Figure 1 online). Thus, dietary Zn levels regulate *miR-31* and *miR-21*

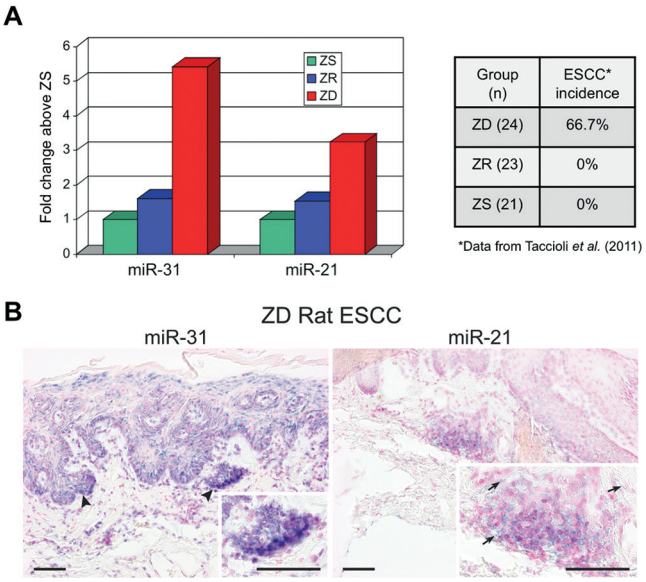

Fig. 4. Correlation of miR-31 and miR-21 expression and ESCC outcome in Zn-modulated rats. (**A**) Taqman miRNA assay showing fold change of miR-31 and miR-21 levels in ZD and ZR (Zn replenished) rats relative to control ZS rats. RNA samples (n = 8 rats/group) were derived from the Taccioli et al. 2011 study (7) (ESCC incidence: ZD rats (16/24, 66.7%), ZR rats (0/23, 0%), ZS rats (0/21, 0%). (**B**) ISH localization of miR-31 and miR-21 in archived ESCC samples from ZD rats (7). miR-31 signal (arrow heads: blue, NBT/BCIP; counterstain, nuclear fast red) was strong/abundant in tumor cells of ESCC from a ZS rat; whereas miR-21 signal (blue, arrows) was mostly in tumor stroma.

expression in esophageal cancer development and prevention; and their dysregulation by ZD is associated with ESCC.

Zn therapy reduces miR-31 and miR-21 expression in rat tongue SCC

Zn supplementation in rats decreased 4-nitroquinoline1-oxide (NQO)-induced tongue SCC incidence and elicited a reduced proliferative/inflammatory cancer phenotype (8). We asked if Zn supplementation that suppresses tongue cancer development also attenuates *miR-31* and *miR-21* expression. ISH analysis was performed on FFPE tissues from NQO-induced rat tongue SCCs with or without Zn therapy (8) (n = 20 rats/Zn treatment group). In near serial sections of these tumor samples (Figure 5, SCC rat tongue), *miR-31* expression was localized to tumor cells, whereas *miR-21* was predominantly found in stromal cells. Importantly, ISH signals of both oncomiRs were reduced in intensity and scope following Zn therapy (Figure 5, ZnSupp versus ZS), thereby showing that their expression is responsive to Zn therapy.

Expression of miR-31 and miR-21 in human tongue SCC

The cellular localization of *miR-31* and *miR-21* in human tongue SCC was determined using ISH (n = 5 cases). As in rat tongue SCC, all five cases of human tongue SCC showed prevalent expression of *miR-31* in tumor cells and *miR-21* expression in stromal cells (Figure 5, SCC human tongue). The ISH data in human and rat tongue SCC (Figure 5) and rat ESCC (Figure 4B) establish that *miR-31* and *miR-21* expression in SCC is cell-type specific, with *miR-31* localized to tumor cells and *miR-21* to tumor stroma.

GO analysis

To gain an understanding of the molecular pathways that are governed by the predicted targets of dysregulated miRNAs in ZD tissues, we performed biological processes enrichment using GO (48). Using target genes found in common in more than two databases (RNAhybrid, TargetScan, miRDB and microRNA.org), we performed GO analysis using DAVID (16) for each of the seven tissues (cutoff

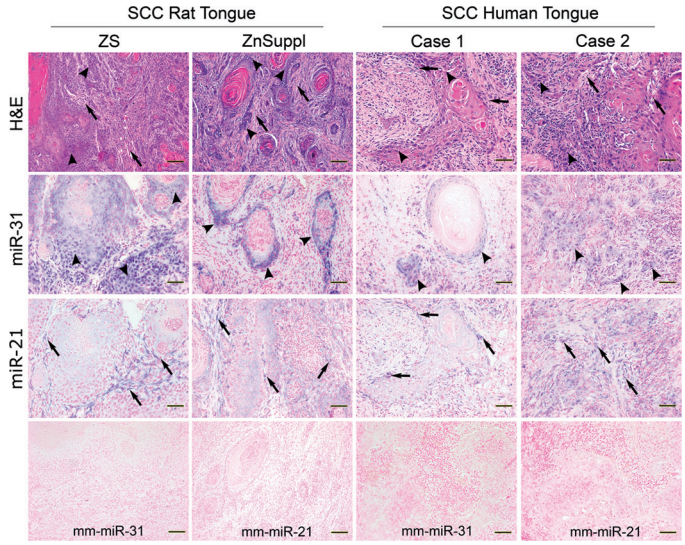

Fig. 5. ISH localization of *miR-31* and *miR-21* in archived rat and human tongue SCCs. Rat tongue SCC: miR-31 signal (arrow heads: blue, NBT/BCIP; counterstain, nuclear fast red) was strong/abundant in tumor cells of proliferative tongue SCC from ZS rats but moderate/infrequent in tumor cells of regressing tongue SCC from Zn-supplemented (ZnSuppl) rats. miR-21 signal (blue, arrows) was strong/abundant in stromal cells of ZS tongue SCC but reduced/infrequent in stromal cells of ZnSuppl tongue SCC. Two cases of human tongue SCC (H&E) are shown: miR-31 signal was predominantly in tumor cells (blue, arrow heads), and miR-21 signal in stroma (blue, arrows). No ISH signal was seen with mm-miR-31 or mm-miR-21 (2 mismatches). miRNA was localized by 4-nitro-blue tetrazolium (NBT) and 5-brom-4-chloro-3′-indolylphosphate (BCIP). Scale bars: 100 μm (H&E, rat tongue SCC; mm-miR-31 and mm-miR-21); 50 μm (miR-31 and miR-21; H&E, human tongue SCC).

of ≥1.3 fold-change and P-value < 0.05). A survey of overrepresented GO terms documented a bias toward genes involved in Zn binding and gene regulatory processes (Table I). In particular, ZD esophagus showed overrepresented processes important in inflammation and cellular proliferation, including serine/threonine-protein kinase activity, MAPKK and JNK cascade and epithelial cell proliferation.

In addition, we performed functional classification of miRNA targets of up- and down-regulated miRNAs in ZD esophagus (see Supplementary Table IV online). The biological processes targeted by the 23 up-regulated miRNAs include processes in inflammation and cell proliferation, namely, serine/threonine-protein kinase activation (40 genes, including tumor suppressors, LATS2 [target of *miR*-31] and MAP2K4 [target of *miR*-31], P = 2.27E-08); regulation of cell motion (27 genes, P = 3.53E-07); and inflammatory response (seven genes, P = 0.028); negative regulation of gene expression (41 genes, including tumor suppressor *PDCD4*; P = 1.10E-04). Importantly, our present study documented a correlation between overexpression of *miR-21* ISH signal (Figure 3B) in the inflammatory ZD esophagus/tongue and loss of expression of its tumor-suppressor target *PDCD4* in the same tissues (Figure 3C). In addition, functional classification of targets of the seven down-regulated miRNAs showed overrepresentation of biological processes such as transcription regulation, negative regulation of gene expression and Zn ion binding.

To determine if these predicted targets of dysregulated miRNAs are relevant to human ESCC development, we retrieved differentially expressed genes (tumor versus normal tissue, P-value < 0.05) from human ESCC/OSCC gene-expression data using ArrayExpress and Gene Expression Omnibus databases. All the selected genes (112 down-regulated and 38 up-regulated, see Supplementary Table V online) belong to the functional families of the predicted targets of dysregulated miRNAs (see Supplementary Table IV online). Interestingly, 47.5% (112 of 236) of our predicted targets for the over-expressed miRNAs are down-regulated in the public ESCC/OSCC gene expression database as compared to 29% (38 of 133) of our predicted targets for the down-regulated miRNAs. Together, our bioinformatics analysis provides a repertoire of putative target genes (see Supplementary Table V online) related to the altered miRNAome of the inflammatory ZD esophagus that may prove to be highly relevant to ESCC development.

Discussion

Dietary ZD increases the risk of ESCC. In a well-established rat model, prolonged ZD causes overexpression of numerous cancer-associated inflammation genes in the esophagus, thus establishing an inflammatory microenvironment that fuels ESCC (7). In the present study, we show that this inflammatory ZD esophagus exhibits a protumorigenic miRNA signature resembling the miRNAomes of human ESCC or OSCC (25–33), with overexpression of five oncogenic miRNAs (*miR-31*, *miR-21*, *miR-223*, *miR-142-3p*, *miR-221*) and down-regulation of two tumor suppressors (*miR-204*, *miR-375*). The data suggest a connection between dysregulation of specific miRNAs and ZD-induced chronic inflammation in esophageal preneoplasia.

In particular, *miR-31* and *miR-21,* the top-up-regulated species in the ZD esophagus, are reported to be elevated in many cancers and inflammation-associated diseases. *miR-21* is one of the most consistently up-regulated oncomiRs in human cancers, and is thought to contribute to inflammation-associated diseases, including cancers (12). *miR-31* is a pleiotropically acting miRNA that is up-regulated in many types of human cancers, including ESCC, tongue SCC, liver cancer and colorectal cancer, but down-regulated in breast metastasis (49). Interestingly, *miR-31* expression levels are reported to increase during inflammatory bowel disease-associated neoplastic transformation (50). Our data show that *miR-21* overexpression in inflammatory ZD esophagus and tongue is correlated with down-regulation of its tumor-suppressor targets *PDCD4* and *TPM1* (Figure 3, B-D). In human ESCC, *miR-21* negatively regulates PDCD4 and knockdown of *miR-21* inhibits cellular proliferation and invasion (51). In ESCC tissues, loss of PDCD4 protein expression is correlated with cancer aggressiveness (tumor stage, nodal metastasis) (52). In tongue SCC tissues, *miR-21* may act as an antiapoptotic factor by blocking *TPM1* expression (45). Although *miR-31* overexpression in ZD esophagus and tongue (Figure 3B) is accompanied by down-regulation of its known tumor-suppressor target *PPP2R2A* (46) (Figure 3D), the role of *PPP2R2A* down-regulation has not been reported in human ESCC or OSCC. We speculate that the down-regulation of such tumor-suppressor targets may relate to the increased cell proliferation and inflammation associated with ZD, as suggested by our GO enrichment analysis of targets of up-regulated miRNAs (see Supplementary Table IV online). The biological role of *miR-21* and *miR-31* in ZD-induced inflammation-associated esophageal carcinogenesis remains to be determined.

Significantly, our present Taqman and ISH data show that *miR-31* and *miR-21* levels were substantially higher in ZD esophagus bearing ESCC versus cancer-free ZS controls (Figure 4 versus Supplementary Figure 1 online). Replenishing Zn reversed the inflammatory gene signature (7) and reduced *miR-31* and *miR-21* levels to ZS levels (Figure 4A, see Supplementary Figure 1 online). Thus, the different ESCC outcome in Zn-modulated animals are directly associated with their elevated and reduced *miR-31* and *miR-21* levels. The data establish for the first time that dietary Zn regulates *miR-31* and *miR-21* expression in ESCC development and prevention.

The tumor-suppressive *miR-375* is known to circulate at low levels in ESCC patients (25), and Ryu et al. (53) showed its acute reversal in serum of Zn-depleted human subjects following a Zn-repletion regimen. The present ISH data that *miR-31* and *miR-21* expression was concomitantly reduced in regressing tongue SCCs from Zn-supplemented rats (8) indicate that these oncomiRs are responsive to Zn therapy (Figure 5). Thus, Zn supplementation may be therapeutic in combating ESCC or OSCC by correcting aberrant miRNA expression. Although Zn therapy inhibits tongue cancer development by suppressing inflammation and cellular proliferation (8), the

mechanism whereby Zn decreases *miR-31* and *miR-21* expression in tongue cancer inhibition needs to be further investigated.

The cellular origins of individual miRNAs are of critical importance in the understanding of the mechanistic roles of miRNAs in tumor development. Whereas *miR*-21 presence in stromal cells of human colorectal (17) and breast cancer (54) was previously reported, the localization of *miR-31* to esophageal/tongue preneoplastic epithelia (Figure 3B) and tumor cells (Figure 4B and Figure 5) is reported here for the first time. Thus, *miR-31* and *miR-21* expression is cell-type specific and may serve as markers in tumor diagnosis and prognosis. In addition, the profiling result that *miR-31* was up-regulated in ZD esophagus and tongue, as well as in PBMC from ZD animals, indicates that *miR-31* may serve as a noninvasive diagnostic marker for a premalignant esophageal/lingual condition. In fact, patients with ESCC or OSCC display high levels of *miR-31* (31,32) as well as *miR-21* (25,30) in tumor tissues and in serum/plasma. Conversely, *miR-21* that was overexpressed in most ZD tissues was not up-regulated in PBMC from ZD animals. This result requires further exploration to determine whether the *miR-21* overexpression in PBMC could arise at later stages of ESCC or OSCC development due to elevation of *miR-21* expression in the tumor stroma (Figure 4B and Figure 5), as compared to stroma of hyperplastic tissues (Figure 3B).

The miRNAomes of the other six inflammatory ZD tissues (Figure 1, B-D) showed dysregulation of specific oncogenic and tumor-suppressor miRNAs (Figure 2C). These changes resemble the hallmarks of the miRNAomes of various human conditions, such as pancreatitis and pancreatic ductal adenocarcinoma (22,38), liver cancer (39), inflammatory COPD and lung cancer (37,38), prostate cancer (40–42), inflammatory human psoriatic skin (34) and PBMC of patients with sepsis (43). Interestingly, patients with these inflammation conditions, namely psoriasis (35), COPD and sepsis (44) are frequently ZD. Thus, ZD modulation of expression of specific miRNAs has implications with regard to the role of ZD in the pathogenesis of these diseases.

With the exception of red meat and seafood, the Zn content in most foods is low. Individuals subsisting largely on a cereal diet are likely to be ZD. Global dietary ZD is estimated to affect 30% of the population, or 4% to 73% across subregions, with higher frequencies occurring in developing countries (55). The mechanistic link to ZD in most disease conditions has remained undefined.

In summary, our present data show that prolonged dietary ZD causes aberrant miRNA expression in a wide variety of tissues associated with inflammation, suggesting a likely mechanism contributing to the burden of human diseases associated with dietary ZD. Importantly, the demonstration of the dysregulation of *miR-31* and *miR-21* by ZD in inflammatory esophageal/lingual neoplasia provides new insight into the mechanisms whereby ZD promotes human ESCC and OSCC.

Supplementary material

Supplementary Tables I, II, III, IV, V and Supplementary Figure 1 can be found at http://carcin.oxfordjournals.org/

Funding

National Institute grants (R01CA118560, R21CA152505 to L.Y.F. and R01CA115965 to C.M.C.).

Acknowledgements

We thank Dr Boye S. Nielsen (Exiqon A/S, Diagnostic Product Development, Vedbaek, Denmark) for valuable reagents and advice on miRNA in situ hybridization.

Conflict of Interest Statement: The authors declare no conflicting financial interests.

References

1. Slaughter,D.P. *et al*. (1953) Field cancerization in oral stratified squamous epithelium; clinical implications of multicentric origin. *Cancer*, **6**, 963–968.
2. Prasad,A.S. *et al*. (1998) Nutritional and zinc status of head and neck cancer patients: an interpretive review. *J. Am. Coll. Nutr.*, **17**, 409–418.
3. Abnet,C.C. *et al*. (2005) Zinc concentration in esophageal biopsy specimens measured by x-ray fluorescence and esophageal cancer risk. *J. Natl. Cancer Inst.*, **97**, 301–306.
4. Berg,J.M. *et al*. (1996) The galvanization of biology: a growing appreciation for the roles of zinc. *Science*, **271**, 1081–1085.
5. Fong,L.Y. *et al*. (2005) Dietary zinc modulation of COX-2 expression and lingual and esophageal carcinogenesis in rats. *J. Natl. Cancer Inst.*, **97**, 40–50.
6. Taccioli,C. *et al*. (2009) Zinc replenishment reverses overexpression of the proinflammatory mediator S100A8 and esophageal preneoplasia in the rat. *Gastroenterology*, **136**, 953–966.
7. Taccioli,C. *et al*. (2011) Dietary zinc deficiency fuels esophageal cancer development by inducing a distinct inflammatory signature. *Oncogene*. doi:10.1038/onc.2011.592. [Epub ahead of print]
8. Fong,L.Y. *et al*. (2011) Zinc supplementation suppresses 4-nitroquinoline 1-oxide-induced rat oral carcinogenesis. *Carcinogenesis*, **32**, 554–560.
9. Ambros,V. (2003) MicroRNA pathways in flies and worms: growth, death, fat, stress, and timing. *Cell*, **113**, 673–676.
10. Bartel,D.P. (2009) MicroRNAs: target recognition and regulatory functions. *Cell*, **136**, 215–233.
11. Calin,G.A. *et al*. (2006) MicroRNA signatures in human cancers. *Nat. Rev. Cancer*, **6**, 857–866.
12. Schetter,A.J. *et al*. (2010) Inflammation and cancer: interweaving microRNA, free radical, cytokine and p53 pathways. *Carcinogenesis*, **31**, 37–49.
13. Geiss,G.K. *et al*. (2008) Direct multiplexed measurement of gene expression with color-coded probe pairs. *Nat. Biotechnol.*, **26**, 317–325.
14. Wyman,S.K. *et al*. (2011) Post-transcriptional generation of miRNA variants by multiple nucleotidyl transferases contributes to miRNA transcriptome complexity. *Genome Res.*, **21**, 1450–1461.
15. Fong,L.Y. *et al*. (2001) Esophageal cancer prevention in zinc-deficient rats: rapid induction of apoptosis by replenishing zinc. *J. Natl. Cancer Inst.*, **93**, 1525–1533.
16. Huang da,W. *et al*. (2009) Systematic and integrative analysis of large gene lists using DAVID bioinformatics resources. *Nat Protoc*, **4**, 44–57.
17. Nielsen,B.S. *et al*. (2011) High levels of microRNA-21 in the stroma of colorectal cancers predict short disease-free survival in stage II colon cancer patients. *Clin. Exp. Metastasis*, **28**, 27–38.
18. Costello,L.C. *et al*. (2005) Zinc and prostate cancer: a critical scientific, medical, and public interest issue (United States). *Cancer Causes Control*, **16**, 901–915.
19. Chang,J. *et al*. (2004) miR-122, a mammalian liver-specific microRNA, is processed from hcr mRNA and may downregulate the high affinity cationic amino acid transporter CAT-1. *RNA Biol.*, **1**, 106–113.
20. Yi,R. *et al*. (2008) A skin microRNA promotes differentiation by repressing "stemness." *Nature*, **452**, 225–229.
21. Poy,M.N. *et al*. (2004) A pancreatic islet-specific microRNA regulates insulin secretion. *Nature*, **432**, 226–230.
22. Szafranska,A.E. *et al*. (2007) MicroRNA expression alterations are linked to tumorigenesis and non-neoplastic processes in pancreatic ductal adenocarcinoma. *Oncogene*, **26**, 4442–4452.
23. Brown,B.D. *et al*. (2006) Endogenous microRNA regulation suppresses transgene expression in hematopoietic lineages and enables stable gene transfer. *Nat. Med.*, **12**, 585–591.
24. Hunter,M.P. *et al*. (2008) Detection of microRNA expression in human peripheral blood microvesicles. *PLoS ONE*, **3**, e3694.
25. Komatsu,S. *et al*. (2011) Circulating microRNAs in plasma of patients with oesophageal squamous cell carcinoma. *Br. J. Cancer*, **105**, 104–111.
26. Lajer,C.B. *et al*. (2011) Different miRNA signatures of oral and pharyngeal squamous cell carcinomas: a prospective translational study. *Br. J. Cancer*, **104**, 830–840.
27. Mathé,E.A. *et al*. (2009) MicroRNA expression in squamous cell carcinoma and adenocarcinoma of the esophagus: associations with survival. *Clin. Cancer Res.*, **15**, 6192–6200.
28. Feber,A. *et al*. (2008) MicroRNA expression profiles of esophageal cancer. *J. Thorac. Cardiovasc. Surg.*, **135**, 255–60.
29. Wong,T.S. *et al*. (2008) Mature miR-184 as Potential Oncogenic microRNA of Squamous Cell Carcinoma of Tongue. *Clin. Cancer Res.*, **14**, 2588–2592.

30. Reis,P.P. *et al*. (2010) Programmed cell death 4 loss increases tumor cell invasion and is regulated by miR-21 in oral squamous cell carcinoma. *Mol. Cancer*, **9**, 238.
31. Zhang,T. *et al*. (2011) The oncogenetic role of microRNA-31 as a potential biomarker in oesophageal squamous cell carcinoma. *Clin. Sci.*, **121**, 437–447.
32. Liu,C.J. *et al*. (2010) Increase of microRNA miR-31 level in plasma could be a potential marker of oral cancer. *Oral Dis.*, **16**, 360–364.
33. Liu,C.J. *et al*. (2010) miR-31 ablates expression of the HIF regulatory factor FIH to activate the HIF pathway in head and neck carcinoma. *Cancer Res.*, **70**, 1635–1644.
34. Joyce,C.E. *et al*. (2011) Deep sequencing of small RNAs from human skin reveals major alterations in the psoriasis miRNAome. *Hum. Mol. Genet.*, **20**, 4025–4040.
35. Michaëlsson,G. *et al*. (1990) Patients with dermatitis herpetiformis, acne, psoriasis and Darier's disease have low epidermal zinc concentrations. *Acta Derm. Venereol.*, **70**, 304–308.
36. Broome,A.M. *et al*. (2003) S100 protein subcellular localization during epidermal differentiation and psoriasis. *J. Histochem. Cytochem.*, **51**, 675–685.
37. Ezzie,M.E. *et al*. (2012) Gene expression networks in COPD: microRNA and mRNA regulation. *Thorax*, **67**, 122–131.
38. Volinia,S. *et al*. (2006) A microRNA expression signature of human solid tumors defines cancer gene targets. *Proc. Natl. Acad. Sci. U.S.A.*, **103**, 2257–2261.
39. Meng,F. *et al*. (2007) MicroRNA-21 regulates expression of the PTEN tumor suppressor gene in human hepatocellular cancer. *Gastroenterology*, **133**, 647–658.
40. Schaefer,A. *et al*. (2010) Diagnostic and prognostic implications of microRNA profiling in prostate carcinoma. *Int. J. Cancer*, **126**, 1166–1176.
41. Sikand,K. *et al*. (2011) miR 488* inhibits androgen receptor expression in prostate carcinoma cells. *Int. J. Cancer*, **129**, 810–819.
42. Lee,K.H. *et al*. (2009) MicroRNA-330 acts as tumor suppressor and induces apoptosis of prostate cancer cells through E2F1-mediated suppression of Akt phosphorylation. *Oncogene*, **28**, 3360–3370.
43. Vasilescu,C. *et al*. (2009) MicroRNA fingerprints identify miR-150 as a plasma prognostic marker in patients with sepsis. *PLoS ONE*, **4**, e7405.
44. Besecker,B.Y. *et al*. (2011) A comparison of zinc metabolism, inflammation, and disease severity in critically ill infected and noninfected adults early after intensive care unit admission. *Am. J. Clin. Nutr.*, **93**, 1356–1364.
45. Li,J. *et al*. (2009) MiR-21 indicates poor prognosis in tongue squamous cell carcinomas as an apoptosis inhibitor. *Clin. Cancer Res.*, **15**, 3998–4008.
46. Liu,X. *et al*. (2010) MicroRNA-31 functions as an oncogenic microRNA in mouse and human lung cancer cells by repressing specific tumor suppressors. *J. Clin. Invest.*, **120**, 1298–1309.
47. Beder,L.B. *et al*. (2006) Identification of a candidate tumor suppressor gene RHOBTB1 located at a novel allelic loss region 10q21 in head and neck cancer. *J. Cancer Res. Clin. Oncol.*, **132**, 19–27.
48. Ashburner,M. *et al*. (2000) Gene ontology: tool for the unification of biology. The Gene Ontology Consortium. *Nat. Genet.*, **25**, 25–29.
49. Valastyan,S. *et al*. (2010) miR-31: a crucial overseer of tumor metastasis and other emerging roles. *Cell Cycle*, **9**, 2124–2129.
50. Olaru,A.V. *et al*. (2011) Dynamic changes in the expression of MicroRNA-31 during inflammatory bowel disease-associated neoplastic transformation. *Inflamm. Bowel Dis.*, **17**, 221–231.
51. Hiyoshi,Y. *et al*. (2009) MicroRNA-21 regulates the proliferation and invasion in esophageal squamous cell carcinoma. *Clin. Cancer Res.*, **15**, 1915–1922.
52. Fassan,M. *et al*. (2010) Programmed cell death 4 protein in esophageal cancer. *Oncol. Rep.*, **24**, 135–139.
53. Ryu,M.S. *et al*. (2011) Genomic analysis, cytokine expression, and microRNA profiling reveal biomarkers of human dietary zinc depletion and homeostasis. *Proc. Natl. Acad. Sci. U.S.A*.
54. Rask,L. *et al*. (2011) High expression of miR-21 in tumor stroma correlates with increased cancer cell proliferation in human breast cancer. *APMIS*, **119**, 663–673.
55. Caulfield,L.E. *et al*. (2004) Zinc deficiency. In M. Ezzati, A.D. Lopez, A. Rodgers and CJ Murray (eds.), *Comparative Quantification of Health Risk*. World Health Organization, Geneva, Switzerland, vol. **1**, pp. 257–280.

Received March 12, 2012; revised May 10, 2012; accepted June 01, 2012